Unmyelinated type II afferent neurons report cochlear damage

Chang Liu[a], Elisabeth Glowatzki[a,b], and Paul Albert Fuchs[a,b,1]

[a]Department of Neuroscience, Johns Hopkins University School of Medicine, Baltimore, MD 21205; and [b]Department of Otolaryngology–Head and Neck Surgery, Johns Hopkins University School of Medicine, Baltimore, MD 21205

In the mammalian cochlea, acoustic information is carried to the brain by the predominant (95%) large-diameter, myelinated type I afferents, each of which is postsynaptic to a single inner hair cell. The remaining thin, unmyelinated type II afferents extend hundreds of microns along the cochlear duct to contact many outer hair cells. Despite this extensive arbor, type II afferents are weakly activated by outer hair cell transmitter release and are insensitive to sound. Intriguingly, type II afferents remain intact in damaged regions of the cochlea. Here, we show that type II afferents are activated when outer hair cells are damaged. This response depends on both ionotropic (P2X) and metabotropic (P2Y) purinergic receptors, binding ATP released from nearby supporting cells in response to hair cell damage. Selective activation of P2Y receptors increased type II afferent excitability by the closure of KCNQ-type potassium channels, a potential mechanism for the painful hypersensitivity (that we term "noxacusis" to distinguish from hyperacusis without pain) that can accompany hearing loss. Exposure to the KCNQ channel activator retigabine suppressed the type II fiber's response to hair cell damage. Type II afferents may be the cochlea's nociceptors, prompting avoidance of further damage to the irreparable inner ear.

type II cochlear afferents | ATP | acoustic trauma | hyperacusis | noxacusis

The mammalian cochlea is the most elaborate of vertebrate auditory organs. The elegantly coiled, mechanically tuned cochlear duct and functional differentiation between inner hair cells (IHCs) and outer hair cells (OHCs), afferent and efferent neuronal connections are among the features that enable the widest acoustic frequency range and most complex vocalizations among vertebrate species. This benefit, however, has been gained at a significant cost in the metabolic and mechanical vulnerability of cochlear hair cells and neurons. Loud sound progressively damages type I afferent neurons and OHCs (1). Once damaged beyond repair, these do not regenerate as they do in nonmammalian vertebrates, suggesting that protective mechanisms should exist to preserve cochlear function. Indeed, middle ear reflexes (2) and efferent inhibition of hair cells (3) can mitigate acoustic trauma to some extent. However, a more effective strategy is simply to avoid or withdraw from sources of trauma, by analogy to limb withdrawal triggered by C-fiber activation in skin.

Here, we provide evidence that unmyelinated type II cochlear afferents can report cochlear trauma, a potential trigger for nocifensive behavior. Hyperactivity of type II neurons could contribute as well to the paradoxical hypersensitivity to loud sound that can accompany hearing loss, despite diminished type I afferent function. Hyperacusis is a comorbidity in 80% of tinnitus patients (4) suggesting common pathogenic mechanisms (5). In the most severe cases, hyperacusis is described as debilitating "ear pain" (6). The response to trauma by type II afferents may relate most directly to such noxious hearing—"noxacusis," to coin a term. In support of this hypothesis, sparse (~5% of all spiral ganglion neurons) unmyelinated type II afferents can survive cochlear damage (7, 8), are insensitive to sound (9, 10), but are activated by the algogenic ligand adenosine triphosphate (ATP) (11). In contrast to the predominant type I afferents that contact IHCs to encode the information content of sound, type II afferents innervate OHCs,

which are more sensitive to acoustic trauma (12). Here, we show that type II afferents are excited by ATP released from supporting cells around damaged OHCs, revealing cellular mechanisms and potential molecular pathways for inner ear pain.

Results

The Experimental Preparation. To monitor type II afferents, intracellular and extracellular recordings were made from their spiral dendrites under OHCs in the apical turn of the cochlea excised from young rats [postnatal day 7 (P7) to P10] (Fig. 1A). As a proxy for cochlear trauma, individual OHCs were ruptured with a glass microneedle positioned apical to the recording electrode. By rapidly advancing the needle, one to three OHCs were ruptured (Fig. 1B), visualized by the loss of FM1-43 fluorescence specifically taken up through hair cells' transduction channels (13) (Fig. 1C). The damaged hair cells become round and swollen, and disintegrate within a few minutes after rupture. Equivalent but off-center punctures failed to rupture hair cells and no change was recorded in type II membrane current or potential, ruling out direct mechanical effects of the needle on the type II afferent (Fig. 2B).

ATP Contributes to the Cell Damage-Induced Response. Upon OHC rupture, a large depolarization (23.8 ± 4.5 mV; 14 trials in seven afferents) was recorded from type II afferents (Fig. 2A). In voltage-clamp recordings, a long-lasting inward current was observed (peak current, 111.9 ± 16.4 pA at -70 mV; 10 trials in six fibers) with a 90% decay time of 58.0 ± 9.5 s. A role for ATP in this response was shown by the application of pyridoxalphosphate-6-azophenyl-2′,4′-disulfonic acid (PPADS) (50 μM), a P2X receptor antagonist that also partially blocks P2Y4 and P2Y6 receptors. The damage-induced current was greatly abbreviated in PPADS (Fig. 2C)

NEUROSCIENCE

mediated by ligand-gated P2X receptors and G-protein–coupled P2Y receptors, respectively.

A voltage-ramp protocol was used to unveil the ionic mechanism underlying ATP- or UTP-evoked current. Ramp current in the absence of ATP or UTP (Fig. 3 C and D, black) was subtracted from that in its presence (Fig. 3 C and D, red and blue) to obtain the ATP- or UTP-dependent ramp current (Fig. 3 C and D, *Inset*). The ATP-dependent current–voltage (*I–V*) relation had a positive slope at its reversal near 0 mV (Fig. 3*E*; representative of five experiments in three cells), consistent with the activation of non-selective cation channels (P2X receptors). In contrast, the UTP-evoked ramp current was entirely inward, activating positive to −70 mV (Fig. 3*F*; representative of six experiments in six cells), suggesting the closure of voltage-dependent potassium channels by P2Y receptors signaling through second-messenger pathways (19).

P2Y Receptors Close KCNQ Channels to Increase Type II Afferent Excitability. The KCNQ channel antagonist XE-991 reversibly eliminated the UTP-dependent ramp current in type II afferents (Fig. 4*A*; from 92.7 ± 20.8 to 3.8 ± 4.5 pA at +40 mV; four experiments in four cells; $P < 0.01$), and the KCNQ channel opener retigabine reliably activated outward currents (Fig. 4*B*; 37.9 ± 3.0 pA at −60 mV; four experiments in four cells). These effects suggest that P2Y receptor activation depolarized type II afferents through the closure of KCNQ channels. This is consistent with the small effect of UTP at −60 mV (Fig. 3*B*) where few voltage-dependent KCNQ channels are open. The relative contribution of P2X and P2Y–KCNQ pathways depends on the local ATP concentration. In submicromolar ATP, the higher-affinity P2Y–KCNQ pathway is preferentially activated. In higher concentrations of ATP, the ionotropic P2X receptors predominate (Fig. S3).

The closure of KCNQ channels by P2Y receptors increased type II fiber excitability. In UTP, the current threshold for type II afferent action potentials was reduced to $78.2 \pm 3.5\%$ of the level required in normal conditions (four experiments in four cells;

Fig. 1. The experimental preparation. (*A*) Whole mount of the apical turn of a P8 rat cochlea (apex to the *Left*), type II afferent filled with biocytin. Typical recording site (arrow) and OHC damage site were within the branched synaptic input zone. (Scale bar: 250 μm.) (*B*) Electrode (*Right*) recording from a type II afferent (out of focus) under OHC rows (stars). The glass needle (arrow) poised to ablate one to three OHCs per trial. (*C*) Two FM1-43–loaded OHCs [arrowheads (*Ci*)] were ruptured and lost fluorescence (*Cii*).

(90% decay time, 13.3 ± 7.9 s; $P < 0.001$ compared with control), and charge transfer decreased (from 2.5 ± 0.4 nC in control to 0.8 ± 0.2 nC; $P < 0.001$). This prolonged response is similar to the time course of ATP-dependent calcium waves observed in cochlear supporting cells after hair cell rupture. These minutes-long waves trigger regenerative ATP release through connexin hemichannels (14–17). Accordingly, when the connexin hemichannel blocker carbenoxolone (CBX) was applied to block ATP release from supporting cells, the type II afferent response to hair cell damage was significantly shortened, with a 90% decay time of 13.8 ± 2.8 s and charge transfer of 0.8 ± 0.1 nC (Fig. 2*D*; $P < 0.001$ for both measures compared with control), suggesting supporting cells as a major source of ATP acting on type II afferents. In contrast, the peak current amplitude in PPADS and CBX was not significantly different from that of control responses. This early peak also was not affected by glutamate receptor block (Fig. S1) but may reflect potassium release from ruptured OHCs acting directly on type II afferents. The amplitude of the early transient was reduced when external potassium was elevated before hair cell rupture, and equivalent inward currents were produced by direct application of 150 mM K^+ saline (mimicking hair cell cytoplasm) (Fig. S2). Such immediate rupture of individual hair cells might occur in vivo (7). More commonly, however, acoustic stress progressively damages OHCs, leading to their eventual death, and is known to increase ATP concentration in cochlear fluids in vivo (18). Thus, the purinergic excitation of type II afferents was examined in greater detail.

Purinergic Receptors in Type II Afferents. Inward current induced in type II afferents by direct application of ATP (50 μM) (55.3 ± 17.7 pA at −60 mV; 10 experiments in seven cells) was significantly reduced by the P2X antagonist, PPADS (Fig. 3*A*; 3.5 ± 3.4 pA; $P < 0.05$, compared with controls; four experiments in four cells). UTP (100 μM), an agonist of P2Y2, P2Y4, and P2Y6 receptors, evoked a small inward current in voltage clamp at −60 mV (8.9 ± 4.7 pA; 12 experiments in eight cells; Fig. 3*B*). These results suggest the presence of two distinct purinergic responses

Fig. 2. ATP contributes to cell damage-induced response. (*A*) OHC ablation depolarized type II afferents and triggered action potentials on the rising phase (*Inset*). (*B*) Representative traces of damage-induced currents (at −70 mV) from five different type II afferents (gray) and the average (black). Identical needle movement that failed to ablate OHCs induced no current (magenta). (*C*) Average ablation-induced current in PPADS (red, three trials in three afferents) compared with average control current from *B*. (*D*) Average ablation-induced current in CBX (blue, five trials in three afferents) compared with control average.
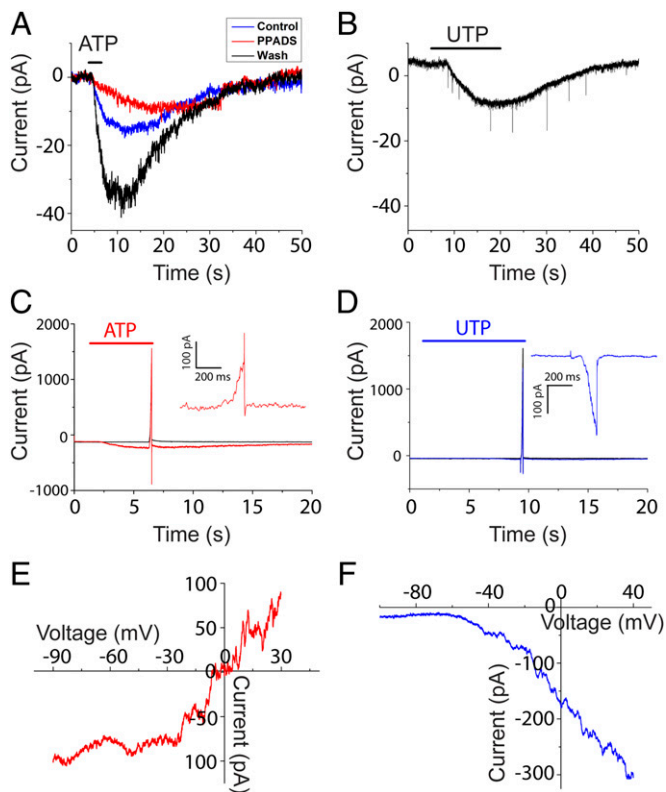
Fig. 3. Purinergic receptors in type II afferents. (*A*) ATP-evoked inward current could be blocked by the P2X antagonist PPADS (red), with partial recovery (blue). (*B*) UTP (agonist for P2Y2 and P2Y4 receptor) induced inward current in type II afferents. Excitatory postsynaptic currents were recorded, but their frequency was not significantly increased during UTP application. (*C*) Overlay of responses from a type II afferent when the holding potential was ramped from −90 to +30 mV in normal external solution (black), or after ATP was applied (red). (*Inset*) Difference current during voltage ramp with and without ATP application. (*D*) Overlay of responses from a type II afferent when the holding potential was ramped from −110 to +30 mV in normal external solution (black), or after UTP was applied (blue). (*Inset*) Difference current during voltage ramp with and without UTP application. (*E* and *F*) I–V relation of ATP and UTP response revealed by voltage-ramp recordings. The current evoked by ATP reversed at 0 mV (red; *n* = 3 afferents) and reversal of UTP-evoked current extrapolated to near −70 mV (blue; *n* = 6 afferents).

$P < 0.01$) (Fig. 4C). Thus, UTP caused a small, but significant increase in excitability, despite the fact that these measurements were made at rest where few KCNQ channels are open (Fig. 3F). The effect of P2Y-mediated KCNQ closure will be greater still when type II afferents are depolarized as during acoustic trauma. Thus, KCNQ channels serve as a promising target to modulate the damage-sensitive type II afferents. Consistent with that proposal, repeated hair cell ablation in the presence of retigabine (KCNQ channel opener) failed to elicit any action potentials in five type II fibers (Fig. 4D), echoing the analgesic effect of retigabine on somatic pain pathways (20).

Discussion

This work provides direct evidence that type II afferents, in addition to sensing glutamate release from OHCs, are activated by cochlear damage in the young rat's cochlea. This observation may help to resolve the decades-long conundrum that type II afferents in vivo are very insensitive to sound (9, 10) and yet presumably carry some information to the auditory brainstem. Likewise, measured ex vivo, synaptic excitation is weak and could activate type II afferents only if all of the presynaptic OHCs were maximally stimulated (21). Alternatively, ATP potently activates type II afferents (11) and

serves as a major contributor to the damage-induced response. ATP can be released into cochlear fluid after tissue stress (even without OHC ablation) in vitro (22) or noise exposure in vivo (18). Experimental ablation of OHCs was shown to initiate ATP-dependent calcium waves in nearby Hensen's cells that further triggers release of ATP through their connexin hemichannels (14–17). P2X2 receptors have been located to the postsynaptic junction in the OHC region in adult guinea pig (23), and P2Y2 receptors have been identified in a small population of spiral ganglion neurons in both adult and neonatal rats (24), suggesting the expression of purinergic receptors in type II neurons. Of interest in this context is the previous report that sensitivity to ATP is reduced in type II afferents after the onset of hearing (11), consistent with the fact that loud sound is not usually painful to normal ears. However, purinergic signaling in the cochlea is up-regulated after noise exposure (25), raising the possibility that type II afferents become more sensitive after damage, in part by increased sensitivity to ATP.

ATP-dependent activation of type II afferents differs from the generation of spontaneous activity in type I afferents by ATP released from cells of Kolliker's organ during cochlear maturation (26). ATP application produced action potentials in type I fibers only via release of glutamate from IHCs, whereas direct effects of ATP on type I afferent membrane current or voltage were small and subthreshold. In contrast, although ATP can evoke glutamate release from OHCs, that source of excitation on its own is insufficient to activate the type II afferent (11, 21).
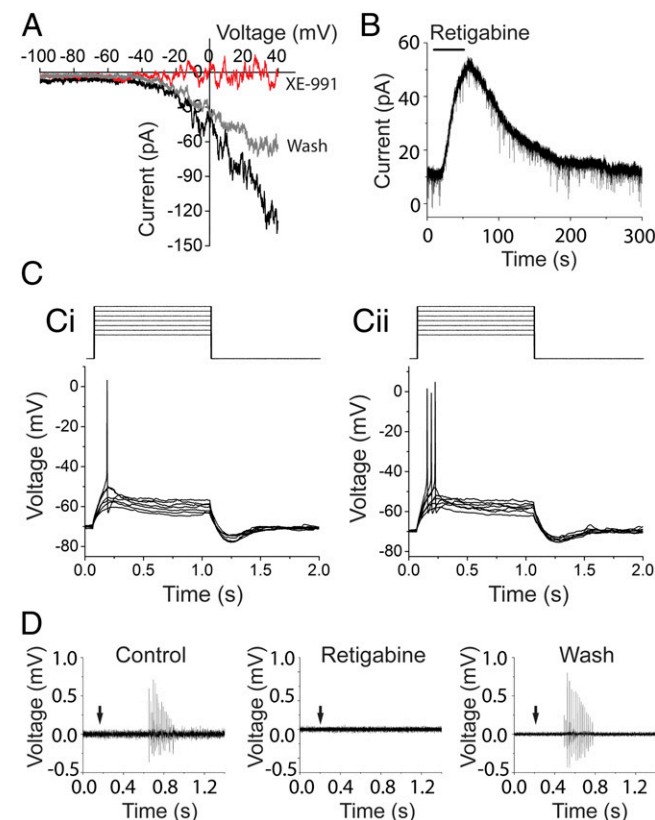

Fig. 4. KCNQ channels regulate type II afferent excitability. (*A*) XE-991 (KCNQ blocker) reversibly eliminated the UTP-evoked ramp current. I–V relation of UTP before (black), during (red), and after (gray) XE-991 application. (*B*) Retigabine (KCNQ opener) induced outward current at −60 mV in type II cochlear afferents. (*C*) Current step protocol (1pA steps) to evoke action potentials (*Ci*). In UTP, from the same resting membrane potential, action potentials were evoked by smaller current steps (*Cii*). (*D*) The KCNQ channel activator retigabine reversibly prevented the response of type II afferents to OHC ablation (*n* = 5 afferents).

Thus, even in the immature cochlea, type II and type I afferents have complementary neurochemical sensitivities. Type I afferents are strongly activated by glutamate release from IHCs, but not by ATP. Type II afferents are strongly activated by ATP, but only weakly by glutamate release from OHCs. These distinctions reinforce the hypothesis that type I and type II afferents serve different functional roles: as acoustic (type I) versus trauma (type II) detectors, by analogy to the differentiation of fine touch and pain afferents in skin. That analogy is reinforced by morphology: larger diameter, myelinated afferents provide analytical sensation (sound, touch), whereas smaller diameter, unmyelinated afferents (cutaneous C fibers, type II cochlear afferents) warn of tissue damage. Somatic C fibers and type II cochlear afferents also share a sensitivity to the algogenic ligand ATP and both can be excited by ATP release during tissue damage (27). Finally, the KCNQ activator retigabine can silence both type II afferents and somatic pain fibers (20).

If type II afferents are nociceptors, then that information should reach central targets mediating withdrawal, or nocifensive behavior, distinct from the standard auditory pathways through inferior colliculus to medial geniculate that serve cognitive hearing. Type I and type II axons arborize in parallel to the dorsal and ventral cochlear nuclei in the brainstem; but only type II endings are found within the small cell cap and granule cell layers that envelope the principal nuclei (28–32). The granule cell domain is thought to be a site for multimodal integration as well as the target of collaterals from olivocochlear efferents (29, 30, 33–38). Whether components of the small cell cap or granule cell layers project to central pain pathways remains to be determined. However, recent work has shown that damaging sound increased activity-dependent c-Fos expression in the granule cell region of the cochlear nucleus (39). It also has been suggested that activation of type II afferents drives medial olivocochlear efferents to suppress cochlear sensitivity (40), although that hypothesis is difficult to reconcile with the fact that medial olivocochlear efferents have acoustic tuning and sensitivity similar to those of type I afferents (41).

Noise-induced cochlear neuropathy can lead to acoustic hypersensitivity (42). Posttraumatic sensitization of damage-resistant type II afferents (7, 8), like the peripheral sensitization of somatic nociceptors in hyperalgesia (43), could contribute to the paradoxical "gain of function" of hyperacusis, whereby loud sound becomes acutely painful even when hearing thresholds are elevated. Hyperacusis and tinnitus are debilitating symptoms that often accompany hearing loss. Tinnitus may result from central nervous system plasticity after afferent loss, by analogy to phantom limb pain, whereas painful hyperacusis—noxacusis—bears similarities to peripheral hypersensitivity and allodynia of damaged skin. Alterations in the relative contributions of type II and type I afferents' activity after hearing loss might contribute to both tinnitus and noxacusis. A reduction in KCNQ channel activity in central neurons has been shown to be important for tinnitus induction (44), and KCNQ activators were found to prevent the development of tinnitus in mice (44, 45). KCNQ activators would be expected to silence type II afferents among other targets. It will be of interest to examine type II fibers in the adult cochlea to determine whether synaptic connections, KCNQ channel expression, purinergic sensitivity, or other aspects of excitability undergo long-term changes after acoustic trauma, identifying therapeutic targets for treatment of noxacusis and other sequelae of hearing loss.

Materials and Methods

Electrophysiological Recordings from Type II Cochlear Afferents. The cochlea was dissected from Sprague–Dawley rat pups (P7–P10) according to a protocol approved by the Johns Hopkins Institutional Animal Care and Use Committee. Each animal was put into deep anesthesia by inhalation of isoflurane (Vedco), ensured by a foot pinch test. Then the animal was decapitated and the temporal bone was removed. The apical turn of the cochlea was dissected for ex vivo recording according to published procedures (46). After removing bone and surrounding tissues, the apical turn of the cochlea was exposed and severed at the modiolus. The stria vascularis and tectorial membrane were removed. The dissected cochlear turn was flattened and secured with an inset pin glued to a coverslip for electrophysiological recordings.

Under a microscope (Carl Zeiss Examiner D1) using differential interference contrast optics, four to six OHCs were removed by a large-diameter glass pipette to expose the dendrites of type II cochlear afferents (11). Tight-seal intracellular recordings or loose-patch extracellular recordings were performed around the terminal region of the fiber (Fig. 1A, arrow), where type II afferents rise to the base of OHCs and form synapses. Extracellular solution contained the following (in mM): 5.8 KCl, 144 NaCl, 1.3 $CaCl_2$, 0.9 $MgCl_2$, 0.7 NaH_2PO_4, 5 glucose, 10 Hepes, pH 7.4. Intracellular solution contained the following (in mM): 135 KCl, 0.1 $CaCl_2$, 3.5 $MgCl_2$, 5 K-EGTA, 5 Hepes, 5 NaCl, pH 7.2 (4-mV junction potential, not corrected). During the voltage-ramp protocol, 1 μM tetrodotoxin was added to the bath to prevent action currents. Pharmacological compounds were applied with a gravity-driven, large-bore application pipette placed to cover the spiral branch of the recorded afferent. All chemical and pharmacological reagents were obtained from Sigma, except for PPADS (Tocris), tetrodotoxin (Tocris), CNQX (Tocris), D-AP5 (Tocris), (RS)-MCPG (Tocris), retigabine (Sigma and Alomone Labs), and FM 1-43FX (Life Technologies). Recording pipettes (resistances of 6–9 MΩ) were pulled from 1-mm borosilicate glass (WPI Instruments). The series resistances of the recordings were less than 35 MΩ (membrane test of the pCLAMP 10.3 software; Molecular Devices) and were not corrected.

Cell ablation was performed mechanically, using a sharp needle pulled from 1-mm borosilicate glass. The needle was placed parallel to the cochlear spiral and was moved manually using a micromanipulator (Sutter Instruments). This ablation procedure started 15–20 OHCs apical to the recording site, to encompass the synaptic zone of the fiber. To visualize hair cell ablation, the cochlear tissue was preloaded (25–30 s; room temperature) with 5 μM FM1-43, a fluorescent dye that rapidly enters through mechanotransduction channels and partitions into the hair cell membrane. In each trial, one to three OHCs were ruptured by the movement of the needle through the lateral wall of the cell (Fig. 1B). Rupture was effected only when the needle was centered on the cell nucleus. After ablation, the damaged OHC swelled immediately and disappeared entirely within 3–5 min, confirmed by the loss of FM1-43 from the hair cell membrane. There was minimal damage to the surrounding cochlear cells including the afferent neurites, Deiters' cells, and Hensen's cells. To improve stability, some recordings were made with intracellular solution containing organic anions in place of Cl (in mM): 110 K-methanesulfonate, 20 KCl, 0.1 $CaCl_2$, 3.5 $MgCl_2$, 5 K-EGTA, 5 Hepes, 5 Na_2-phosphocreatine, 0.3 Tris-GTP, pH 7.2. Membrane potentials were corrected for the 10-mV junction potential with this solution.

Data Acquisition and Analysis. Membrane voltage and current were recorded with a MultiClamp 700B amplifier and a Digidata 1440A (Molecular Devices), controlled by pCLAMP 10.3 software (Molecular Devices), sampled at 25 kHz, and low-pass filtered at 10 kHz. The data were analyzed in pCLAMP 10.3 (Molecular Devices) and Origin 9.0 (Origin Labs). Statistical analysis (paired or unpaired t test as appropriate) was performed in Excel (Microsoft), and the results are given as mean ± SD.

Post Hoc Visualization of Biocytin-Filled Type II Afferents. For post hoc visualization of the afferent, 2.5–3.0 mg/mL biocytin was added to intracellular solution. The tracer was detected using streptavidin-conjugated horseradish peroxidase, made visible by precipitation of diaminobenzidine (DAB) for light microscopy. After whole-cell patch-clamp recording, tissue with biocytin-filled type II afferents was fixed in 4% (vol/vol) PFA overnight at 4 °C, and stored in PBS for further processing within 2 wk. The tissue was quenched in 10% H_2O_2 [with 10% (vol/vol) methanol] for 10 min, and permeabilized in 2% Triton in PBS (1 h; room temperature). Then the tissue was incubated in avidin/biotin complex (Vectastain ABC kit; Vector) overnight at 4 °C, washed in PBS, and reacted with a DAB-based peroxide substrate (ImmPACT DAB; Vector) for 10 min, until the cell and its arborization were visible under the microscope. The tissue was mounted on a slide for imaging.

Equipment and Settings for Digital Images. After the DAB reaction, the slides for cochlea turns were imaged on a Zeiss LSM 510 Meta microscope. For cell ablation studies, the cochlea was viewed under a microscope (Carl Zeiss Examiner D1) using a 40× water-immersion objective with contrast enhancement (Hamamatsu C2400-62). Images were taken with a digital camera (Sony) attached to the microscope.

1. Wong AC, Ryan AF (2015) Mechanisms of sensorineural cell damage, death and survival in the cochlea. *Front Aging Neurosci* 7:58.
2. Brask T (1979) The noise protection effect of the stapedius reflex. *Acta Otolaryngol Suppl* 360:116–117.
3. Guinan JJ, Jr (2006) Olivocochlear efferents: Anatomy, physiology, function, and the measurement of efferent effects in humans. *Ear Hear* 27(6):589–607.
4. Dauman R, Bouscau-Faure F (2005) Assessment and amelioration of hyperacusis in tinnitus patients. *Acta Otolaryngol* 125(5):503–509.
5. Hébert S, Fournier P, Noreña A (2013) The auditory sensitivity is increased in tinnitus ears. *J Neurosci* 33(6):2356–2364.
6. Pienkowski M, et al. (2014) A review of hyperacusis and future directions: Part II. Measurement, mechanisms, and treatment. *Am J Audiol* 23(4):420–436.
7. Spoendlin H (1971) Primary structural changes in the organ of Corti after acoustic overstimulation. *Acta Otolaryngol* 71(2):166–176.
8. Ryan AF, Woolf NK, Bone RC (1980) Ultrastructural correlates of selective outer hair cell destruction following kanamycin intoxication in the chinchilla. *Hear Res* 3(4):335–351.
9. Robertson D (1984) Horseradish peroxidase injection of physiologically characterized afferent and efferent neurones in the guinea pig spiral ganglion. *Hear Res* 15(2):113–121.
10. Brown MC (1994) Antidromic responses of single units from the spiral ganglion. *J Neurophysiol* 71(5):1835–1847.
11. Weisz C, Glowatzki E, Fuchs P (2009) The postsynaptic function of type II cochlear afferents. *Nature* 461(7267):1126–1129.
12. Liberman MC, Kiang NY (1978) Acoustic trauma in cats. Cochlear pathology and auditory-nerve activity. *Acta Otolaryngol Suppl* 358:1–63.
13. Meyers JR, et al. (2003) Lighting up the senses: FM1-43 loading of sensory cells through nonselective ion channels. *J Neurosci* 23(10):4054–4065.
14. Gale JE, Piazza V, Ciubotaru CD, Mammano F (2004) A mechanism for sensing noise damage in the inner ear. *Curr Biol* 14(6):526–529.
15. Piazza V, Ciubotaru CD, Gale JE, Mammano F (2007) Purinergic signalling and intercellular Ca^{2+} wave propagation in the organ of Corti. *Cell Calcium* 41(1):77–86.
16. Anselmi F, et al. (2008) ATP release through connexin hemichannels and gap junction transfer of second messengers propagate Ca^{2+} signals across the inner ear. *Proc Natl Acad Sci USA* 105(48):18770–18775.
17. Lahne M, Gale JE (2010) Damage-induced cell-cell communication in different cochlear cell types via two distinct ATP-dependent Ca waves. *Purinergic Signal* 6(2):189–200.
18. Muñoz DJ, Kendrick IS, Rassam M, Thorne PR (2001) Vesicular storage of adenosine triphosphate in the guinea-pig cochlear lateral wall and concentrations of ATP in the endolymph during sound exposure and hypoxia. *Acta Otolaryngol* 121(1):10–15.
19. Lechner SG, Boehm S (2004) Regulation of neuronal ion channels via P2Y receptors. *Purinergic Signal* 1(1):31–41.
20. Brown DA, Passmore GM (2009) Neural KCNQ (Kv7) channels. *Br J Pharmacol* 156(8):1185–1195.
21. Weisz CJ, Lehar M, Hiel H, Glowatzki E, Fuchs PA (2012) Synaptic transfer from outer hair cells to type II afferent fibers in the rat cochlea. *J Neurosci* 32(28):9528–9536.
22. Zhao HB, Yu N, Fleming CR (2005) Gap junctional hemichannel-mediated ATP release and hearing controls in the inner ear. *Proc Natl Acad Sci USA* 102(51):18724–18729.
23. Housley GD, et al. (1999) Expression of the $P2X_2$ receptor subunit of the ATP-gated ion channel in the cochlea: Implications for sound transduction and auditory neurotransmission. *J Neurosci* 19(19):8377–8388.
24. Huang LC, Thorne PR, Vlajkovic SM, Housley GD (2010) Differential expression of P2Y receptors in the rat cochlea during development. *Purinergic Signal* 6(2):231–248.
25. Wang JC, et al. (2003) Noise induces up-regulation of P2X2 receptor subunit of ATP-gated ion channels in the rat cochlea. *Neuroreport* 14(6):817–823.
26. Tritsch NX, Yi E, Gale JE, Glowatzki E, Bergles DE (2007) The origin of spontaneous activity in the developing auditory system. *Nature* 450(7166):50–55.
27. Cook SP, McCleskey EW (2002) Cell damage excites nociceptors through release of cytosolic ATP. *Pain* 95(1-2):41–47.
28. Brown MC, Berglund AM, Kiang NY, Ryugo DK (1988) Central trajectories of type II spiral ganglion neurons. *J Comp Neurol* 278(4):581–590.
29. Brown MC, Liberman MC, Benson TE, Ryugo DK (1988) Brainstem branches from olivocochlear axons in cats and rodents. *J Comp Neurol* 278(4):591–603.
30. Benson TE, Brown MC (2004) Postsynaptic targets of type II auditory nerve fibers in the cochlear nucleus. *J Assoc Res Otolaryngol* 5(2):111–125.
31. Brown MC, Ledwith JV, 3rd (1990) Projections of thin (type-II) and thick (type-I) auditory-nerve fibers into the cochlear nucleus of the mouse. *Hear Res* 49(1-3):105–118.
32. Hurd LB, Hutson KA, Morest DK (1999) Cochlear nerve projections to the small cell shell of the cochlear nucleus: The neuroanatomy of extremely thin sensory axons. *Synapse* 33(2):83–117.
33. Benson TE, Brown MC (1990) Synapses formed by olivocochlear axon branches in the mouse cochlear nucleus. *J Comp Neurol* 295(1):52–70.
34. Paloff AM, Usunoff KG (1992) Projections to the inferior colliculus from the dorsal column nuclei. An experimental electron microscopic study in the cat. *J Hirnforsch* 33(6):597–610.
35. Wright DD, Ryugo DK (1996) Mossy fiber projections from the cuneate nucleus to the cochlear nucleus in the rat. *J Comp Neurol* 365(1):159–172.
36. Zhan X, Ryugo DK (2007) Projections of the lateral reticular nucleus to the cochlear nucleus in rats. *J Comp Neurol* 504(5):583–598.
37. Shore SE, Zhou J (2006) Somatosensory influence on the cochlear nucleus and beyond. *Hear Res* 216-217:90–99.
38. Brown MC, Pierce S, Berglund AM (1991) Cochlear-nucleus branches of thick (medial) olivocochlear fibers in the mouse: A cochleotopic projection. *J Comp Neurol* 303(2):300–315.
39. Flores EN, et al. (2015) A non-canonical pathway from cochlea to brain signals tissue-damaging noise. *Curr Biol* 25(5):606–612.
40. Froud KE, et al. (2015) Type II spiral ganglion afferent neurons drive medial olivocochlear reflex suppression of the cochlear amplifier. *Nat Commun* 6:7115.
41. Liberman MC, Brown MC (1986) Physiology and anatomy of single olivocochlear neurons in the cat. *Hear Res* 24(1):17–36.
42. Hickox AE, Liberman MC (2014) Is noise-induced cochlear neuropathy key to the generation of hyperacusis or tinnitus? *J Neurophysiol* 111(3):552–564.
43. Treede RD, Meyer RA, Raja SN, Campbell JN (1992) Peripheral and central mechanisms of cutaneous hyperalgesia. *Prog Neurobiol* 38(4):397–421.
44. Li S, Choi V, Tzounopoulos T (2013) Pathogenic plasticity of Kv7.2/3 channel activity is essential for the induction of tinnitus. *Proc Natl Acad Sci USA* 110(24):9980–9985.
45. Kalappa BI, et al. (2015) Potent KCNQ2/3-specific channel activator suppresses in vivo epileptic activity and prevents the development of tinnitus. *J Neurosci* 35(23):8829–8842.
46. Glowatzki E, Fuchs PA (2002) Transmitter release at the hair cell ribbon synapse. *Nat Neurosci* 5(2):147–154.

NEUROSCIENCE